Geologica Acta: an international earth science journal
ISSN: 1695-6133
geologica-acta@ija.csic.es
Universitat de Barcelona
España

OSORIO-GRANADA, E.; RESTREPO-MORENO, S.A.; MUÑOZ-VALENCIA, J.A.; TREJOS- TAMAYO, R.A.; PARDO-TRUJILLO, A.; BARBOSA-ESPITIA, A.A.
Detrital zircon typology and U/Pb geochronology for the Miocene Ladrilleros-Juanchaco sedimentary sequence, Equatorial Pacific (Colombia): New constraints on provenance and paleogeography in northwestern South America
Geologica Acta: an international earth science journal, vol. 15, núm. 3, septiembre, 2017, pp. 201-215
Universitat de Barcelona
Barcelona, España

Geologica Acta, Vol.15, Nº 3, September 2017, 201-215
DOI: 10.1344/GeologicaActa2017.15.3.4

geologica acta

Detrital zircon typology and U/Pb geochronology for the Miocene Ladrilleros-Juanchaco sedimentary sequence, Equatorial Pacific (Colombia): New constraints on provenance and paleogeography in northwestern South America

E. OSORIO-GRANADA[1] S.A. RESTREPO-MORENO[2,3] J.A. MUÑOZ-VALENCIA[1] R.A. TREJOS- TAMAYO[1] A. PARDO-TRUJILLO[1] A.A. BARBOSA-ESPITIA[1,3]

[1]Universidad de Caldas, Facultad de Ciencias, Departamento de Ciencias Geológicas
Grupo de Investigaciones en Estratigrafía y Vulcanología (GIEV-Cumanday), Instituto de Investigaciones en Estratigrafía (IIES), Manizales, Colombia. Pardo-Trujillo E-mail: andres.pardo@ucaldas.edu.co

[2]Departamento de Geociencias y Medio Ambiente, Universidad Nacional de Colombia
Sede Medellín Restrepo Moreno E-mail: sarestrepom@unal.edu.com

[3]Department of Geological Sciences. University of Florida
Gainesville, Florida 32611, USA Barbosa-Espitia E-Mail: angelbarbosa@ufl.edu Restrepo-Moreno E-mail: sergiorm@ufl.edu

ABSTRACT

Typology and internal texture analyses were performed on detrital zircons obtained from the Miocene sandstones of the Ladrilleros-Juanchaco sedimentary sequence (Colombia, Equatorial Pacific). This analysis was complemented with zircon U/Pb dating to identify typology-age associations as indicators of sediment provenance. Our results show that zircons with S and P dominant typologies have internal structures/zoning indicative of igneous, and potentially also metamorphic, origins. Morphometric results suggest limited transport from source areas. Both typology and U/Pb data point to the western Cordillera as the principal source of detrital materials for this sedimentary sequence. A paleogeographic reconstruction shows that, during the Late Miocene, significant portions of the western Cordillera were uplifted and actively eroding, thereby forming a fluvio-topographic barrier that prevented sediments from the central Cordillera reaching the Pacific basins. Exhumed Miocene plutons located along the axis of the western Cordillera may also have played a role as geomorphologically active massifs. This study demonstrates that typologic analysis on detrital zircon grains is a useful tool for establishing provenance and paleogeography in complex litho-tectonic areas where overlapping U/Pb signatures can lead to contradictory results..

KEYWORDS **Miocene. Ladrilleros-Juanchaco sedimentary sequence. Colombia western Cordillera. Provenance.**

INTRODUCTION

Provenance studies in terrigenous sedimentary sequences are crucial for paleogeographic and morpho-tectonic reconstructions (*e.g.,* uplift-erosion, paleotopography, paleofluvial networks, etc.) in mountain ranges and associated sedimentary basins (Pettijohn, 1975; Dickinson, 1985; Bernet and Spiegel, 2004; Garzanti *et al.*, 2007). In recent decades, the study of heavy mineral fractions, geochronology of detrital phases (*e.g.,* U/Pb dating of zircon), and geochemical analysis of detrital materials (trace elements and isotopes) have been incorporated into provenance studies to provide valuable data on the configuration of source areas and their proximity to depositional environments (Armstrong-Altrin *et al.*, 2004; Belousova *et al.*, 2005; Boggs, 2009; Dostal and Keppie, 2009; Etemad-Saeed *et al.*, 2011; Grimes *et al.*, 2015).

Although rock fragments (lithics) and individual mineral grains are excellent indicators of source area, several problems can arise during interpretation. These are related primarily to the lithological and/or compositional similarities between different source areas and to the biased distribution of detrital materials in the sedimentary rock due to the different responses of each fragment/mineral to weathering, erosion, transport, and/or diagenesis (Boggs, 2009). One approach to overcoming these limitations is to use zircons found in the sedimentary rocks. Being chemically and physically refractory, zircon is an ultra-stable mineral phase that is capable of enduring multiple geological cycles in sedimentary, metamorphic and/or igneous environments (Garzanti *et al.*, 1987; Finch and Hanchar, 2003; Hanchar and Hoskin, 2003; Mange and Wright, 2007; Gehrels, 2012, 2014). At present, zircons are employed as key source indicators, based on age of the parental rock through radiometric dating or age of cooling events via thermochronology (Bernet and Spiegel, 2004; Carrapa, 2010; Thomas, 2011; Garver, 2014; Gehrels, 2014). The relatively recent development of dating techniques (*e.g.,* U/Pb via LA-ICP-MS) that can target specific regions within a single crystal has enabled space-explicit dating of complex multiphase zircon grains, while reducing analytical costs and increasing data throughput as several hundred grains in detrital samples can be analyzed in a short time (Bowring and Schmitz, 2003; Davis *et al.*, 2003; Košler and Sylvester, 2003; Bernet and Spiegel, 2004; Schoene, 2014). Thus, in the last decade, U/Pb age spectra in detrital zircons has been used widely to improve constraint of source areas (Thomas, 2011; Gehrels, 2014). Nonetheless, U/Pb age signatures have been shown to be problematic in regions where there is high litho-structural complexity, such as age overlaps between different geological provinces, multiple litho-tectonic blocks with similar lithologies/ages, etc. (Reiners *et al.*, 2005; Carrapa, 2010). One such region is the northern Andes in Colombia (Restrepo and Toussaint, 1988; Toussaint, 1995; Cediel *et al.*, 2003; Moreno-Sánchez and Pardo-Trujillo, 2003) (Figs. 1; 2), where similar U/Pb datasets have resulted in contradictory interpretations (*e.g.,* Montes *et al.*, 2015; O'Dea *et al.*, 2016).

Another approach to studying zircons that have been part of the erosive cycle (*i.e.,* eroded, reworked, and redeposited in sedimentary sequences) is the analysis of different typologies, such as crystal form, degree of elongation, and coloration (Fedo *et al.*, 2003; Anani *etal.*, 2011; Zoleikhaei *et al.*, 2016). Typology of zircon populations (morphology and color) is controlled by the physical and chemical conditions during crystallization (Anani *et al.*, 2011). Morphologic and chromatic features can be examined at high resolution under a petrographic microscope (transmitted and reflected light), and can be associated with the various lithologies present in source areas (Dabard *et al.*, 1996).

In addition to the conventional characterization of zircon morphology by visual inspection under an optical microscope, the development of high-resolution Scanning Electron Microscopy and Cathodoluminescence (SEM-CL) enables us to characterize the internal structure and zonation patterns for each zircon grain dated in a detrital sample, further facilitating the discrimination of igneous and metamorphic zircons, as well as zircons with complex histories (Hanchar and Rudnick, 1995; Corfu *et al.*, 2003). The combination of different techniques such as U/Pb dating and zircon typological analysis, together with internal texture analysis using SEM-CL, is conducive to more robust studies in terms of the discrimination of source areas (Loi and Dabard, 1997; Willner *et al.*, 2003; Anani *et al.*, 2012); an approach strongly needed in complex litho-structural domains such as the Northern Andes (Restrepo-Moreno *et al.*, 2015).

In this work we carry out a detailed analysis of detrital zircons from the Ladrilleros-Juanchaco Sedimentary Sequence (LJSS) based on external and internal zircon morphology using optical (Gärtner *et al.*, 2013) and SEM-CL (Corfu *et al.*, 2003) microscopy. This approach is complemented with zircon chromatic analysis (Pupin and Turco, 1972b; Pupin, 1980; Velez *et al.*, 2005; Shahbazi *et al.*, 2014) and zircon U/Pb dating by LA-ICP-MS (Košler and Sylvester, 2003; Chang *et al.*, 2006; Solari and Tanner, 2011; Schoene, 2014).

The combination of these techniques provides a robust methodological approach to discriminate among zircons on the basis of more than just their radiometric age and external and internal morphology, thus allowing us to determine the age and conditions of zircon formation in the crystalline source (igneous vs. metamorphic) (Poldevaart, 1950; Pupin and Turco, 1972b; Pupin *et al.*, 1978; Pupin, 1988; Corfu *et al.*, 2003). These multi-technique approach is applicable to detrital zircons, enhancing the accuracy in the determination of source areas (Loi and Dabard, 1997; Willner *et al.*, 2003; Anani *et al.*, 2012; Shahbazi *et al.*, 2014).

STUDY AREA

The LJSS is located in northwestern South America on the Equatorial Pacific coastline, at ~5°N latitude.

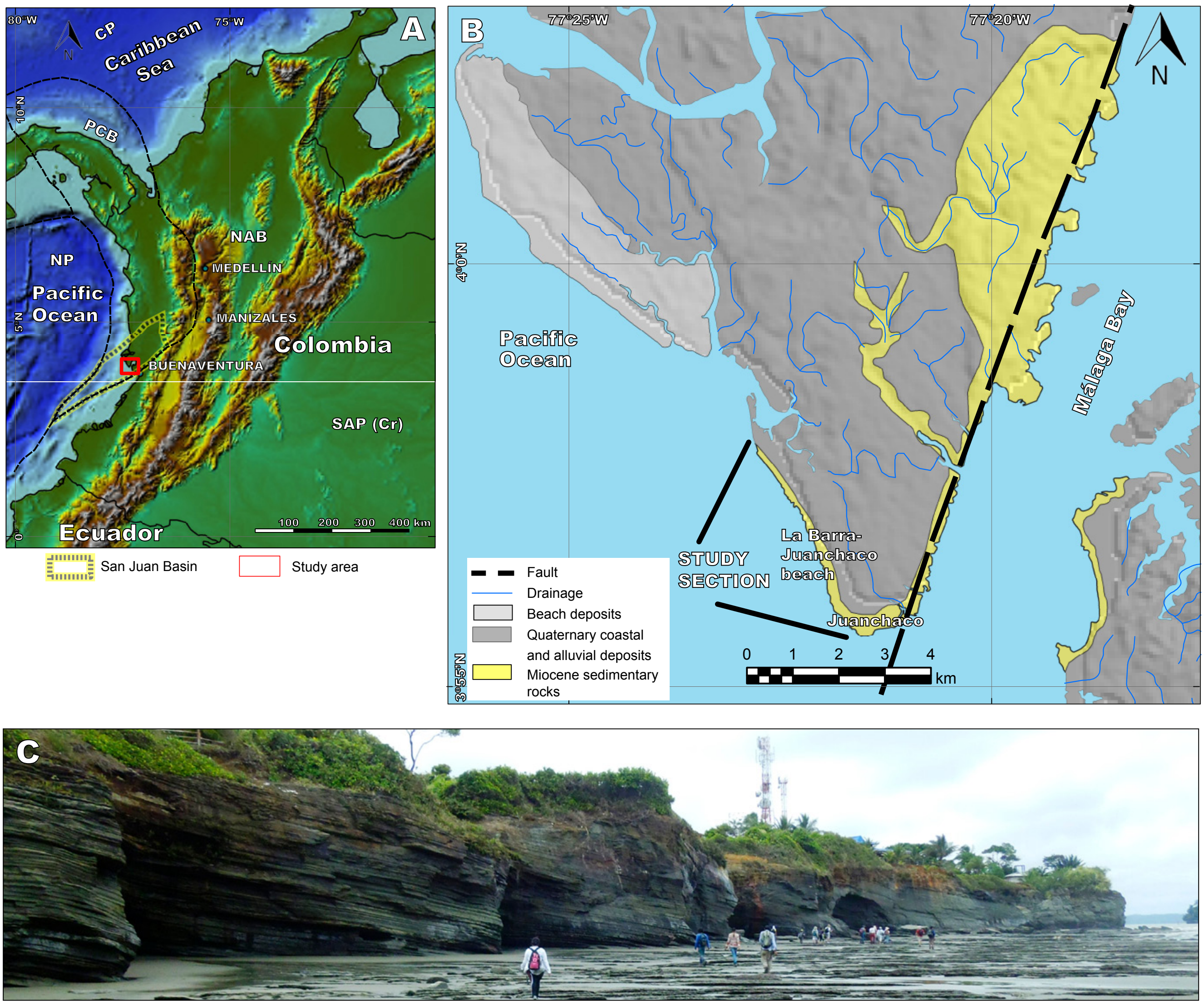

FIGURE 1. A) Location of the Ladrilleros-Juanchaco Sedimentary Sequence (LJSS) on the Colombian and South American context on the Pacific coast. The general geodynamic setting is also shown with main tectonic plates and crustal blocks marked as CP: Caribbean Plate, NP: Nazca Plate, SAP-Cr: South American Plate and Craton, PCB: Panamá-Chocó Block, NAB: Nor-Andean Block (from Suter *et al.*, 2008; Taboada *et al.*, 2000; Cediel *et al.*, 2003). B) Local geological framework of the LJSS (modified from Montoya, 2003). C) General aspect of outcrops for the LJSS in the studied section, NW-SE.

Strata of this sequence outcrop in coastal cliffs along La Barra-Juanchaco Beach and Malaga Bay, approximately 40 km northwest of the city of Buenaventura (Fig. 1). Physiographically, the LJSS occupies a littoral position on the Pacific lowlands to the west of the western Cordillera and to the south of the Serranía Baudó. The LJSS is part of the San Juan Sub-basin that, from a stratigraphic and deep marine deposits sedimentary point of view, is correlated with deep marine deltaic activity (ANH-Universidad de Caldas, 2011). The main modern fluvial system in the area, the Río San Juan, drains the western flank of the western Cordillera to form one of the largest deltaic systems of the South American Equatorial Pacific (González and Correa, 2001).

Litho-structurally, the LJSS (Figs. 1; 2) lies within a tectonic setting known as the Panamá-Choco Block (PCB) and is part of the San Juan Sub-basin, delimited to the south by the Garrapatas fault system and to the north by the San Juan fault system (Cediel *et al.*, 2003, 2009). The regional geodynamic framework is marked by the interaction of major tectonic plates (Nazca, Cocos, Caribbean and South America) in a combined subduction and collision convergent regimen (Kellogg and Bonini, 1982; Kellogg, 1984; Taboada *et al.*, 2000; Spikings *et al.*, 2001; Pindell *et al.*, 2005; Bayona *et al.*, 2011; Pindell and Kennan, 2013). Smaller lithospheric/crustal blocks like the PCB and the Nor-Andean Block (NAB) (Fig.1) also play an important role in the litho-tectonic configuration of the area. The PCB, for instance, is associated with the last collisional episode in the region from Oligocene to present times (Duque-Caro, 1990; Farris *et al.*, 2011).

Previous studies indicate that the LJSS consists of a continuous, well-exposed sequence of clastic materials, such as mudstones with sandstone intercalations, deposited in a marine environment (ANH-Universidad de Caldas, 2011). The sequence is approximately 750m thick (Fig. 3), although Miocene beds can reach thicknesses of >3000m (Cediel *et al.*, 2003). The sedimentary fill of the basin rests on oceanic rocks typical of Colombia's western crustal domain, west of the Cauca-Romeral fault, *i.e.*, the Provincia Litosférica Oceánica Cretácico Occidental (PLOCO) (Gómez *et al.*, 2015). According to Muñoz and Gómez (2014), the LJSS sandstones correspond to lithic arkoses, feldspathic litharenites, and litharenites that are texturally (clay matrix, poor selection, and grain angularity) and compositionally immature. These sandstones are also characterized by a significant input of volcaniclastic

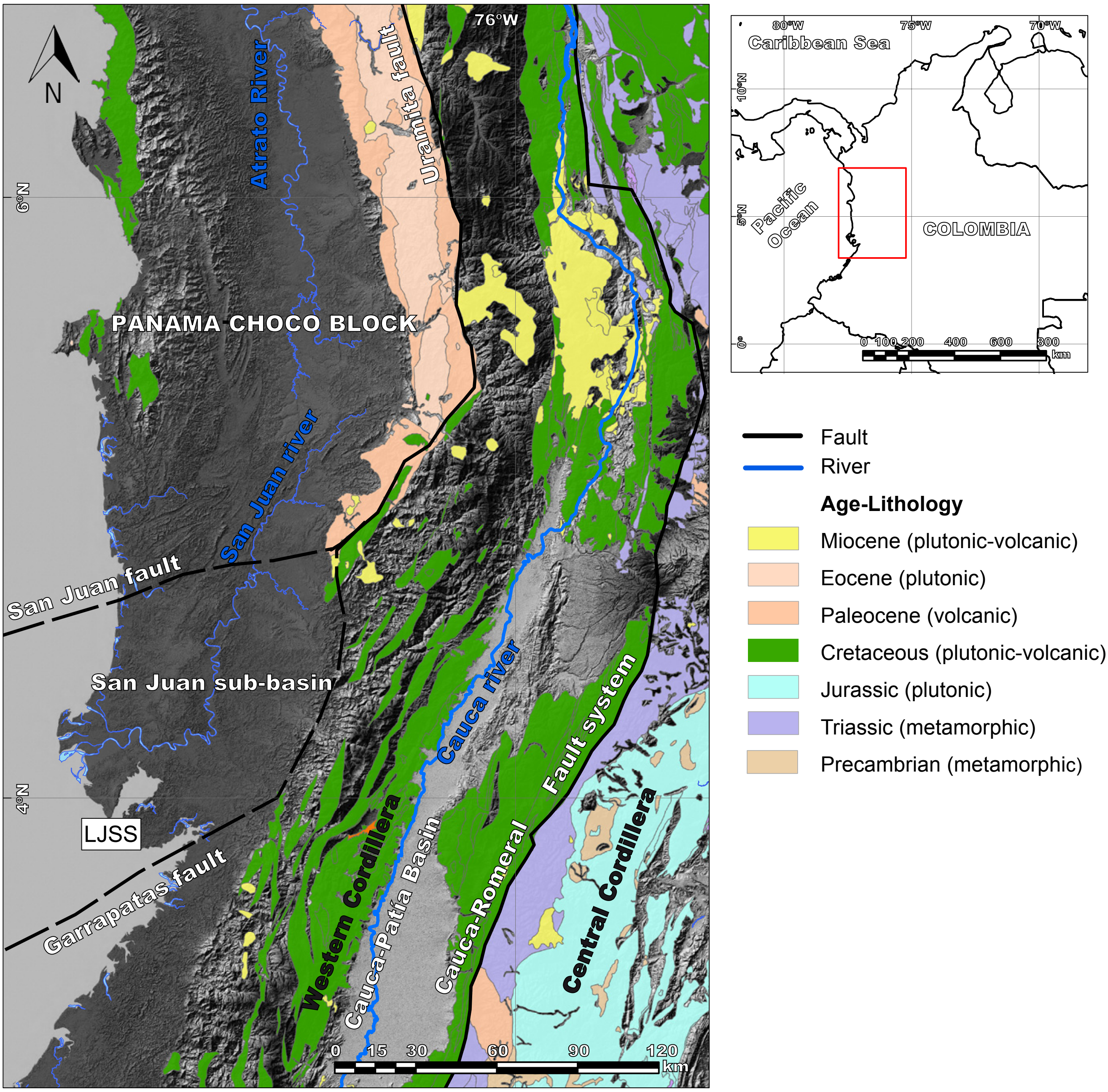

FIGURE 2. Main physiographic, structural, and chrono-stratigraphic framework (igneous and metamorphic units), adjacent to the Ladrilleros-Juanchaco Sedimentary Sequence (LJSS). Non-colored areas represent sedimentary rocks and Quaternary deposits. Modified from Gómez *et al.* (2015).

materials (volcanic fragments, horblende + pyroxene associations, long and euhedral zircon grains) and other detrital components (quartz, metamorphic fragments(?), etc.). The presence of volcanic elements affords the opportunity not only to constrain the age of the sequence but to discriminate among source areas associated with either volcano-magmatic arcs (ages varying between the Cretaceous and the Miocene) or metamorphic elements that can be related to mountain ranges with metamorphic basement rocks such as the central Cordillera (Muñoz and Gómez, 2014). A Burdigalian-Tortonian age (~16-10Ma) has been established for this sedimentary unit based on calcareous microfossils (Vallejo *et al.*, 2016). To date, no geochronological dataset has been used to constrain the age of the LJSS.

Based on a combined analysis of zircon typology, internal textures/zonation patterns and U/Pb dating, our work improves the dating resolution of the sequence, establishes the origin of detrital components, and identifies the paleogeographic conditions that lead to the development of the LJSS.

METHODS

Eleven sandstone samples were collected along various stratigraphic levels of the LJSS to separate zircon grains for typological analysis (Fig. 3). An additional sample was collected from the top of the sequence for LA-ICP-MS U/Pb dating and the generation of age spectra, as well as to determine internal zircon zonation patterns through SEM-CL imagery. All zircon grains were separated by gravimetric methods combining Wilfley® table/gold pan and heavy liquid runs (TBE: 2.96g/cm^3). Mineral concentrates were further purified through additional heavy liquid (MeI: 3.32g/cm^3) and Frantz® Isodynamic magnetic separations. Zircon grains were mounted in cylindrical resin plugs (2cm diameter, 1cm thick) for their subsequent preparation (grinding and polishing to expose internal areas) for U/Pb dating. To ensure a random, unbiased assembly of zircon grains from detrital samples, we emptied ~200-300 grains directly from the vial. Finally, we obtained petrographic and SEM-CL microscopy images of the zircons to reveal the external morphology and chromatic features and to examine internal zonation patterns, respectively.

To assess zircon typology, we implemented the methodology of Pupin (1980) and Gärtner *et al.* (2013) to correlate the analyzed zircons with source area lithologies (*e.g.,* plutonic, volcanic and/or metamorphic), while providing information in terms of multi-cycle zircons. To characterize zircon crystals based on morphology/typology, the following steps were undertaken after Pupin and Minéraux (1976), Pupin (1980), and Gärtner *et al.*

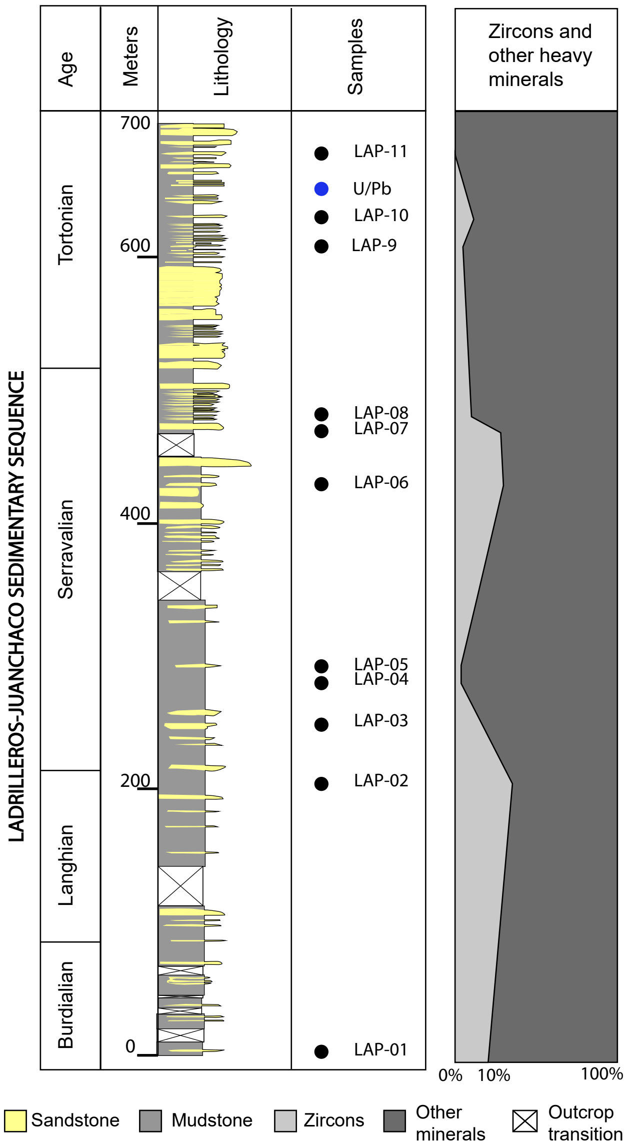

FIGURE 3. Stratigraphic column for the Ladrilleros-Juanchaco sedimentary sequence (adapted from Muñoz and Gómez, 2014). Zircon abundance relative to other heavy minerals is shown. Black dots correspond to the stratigraphic position of samples analyzed. Blue dot marks the position of the sample for detrital zircon U/Pb analysis.

(2013): i) Scanning of grain mounts under the optical microscope to identify ~150 grains of detrital zircon; ii) zircon grain characterization by specific morphometric parameters, such as elongation, roundness, length/width ratios, and degree of face development; iii) zircon grain characterization by color tones and intensity (*e.g.,* hue, saturation, and brightness) and degree of transparency; iv) zircon classification (Fig. 4); v) statistical calculations to quantify variability along the morphometric correlation matrices for each sample; vi) generate specific typological classifications. Microscopic analyses under transmitted and reflected light were carried out at the Instituto de

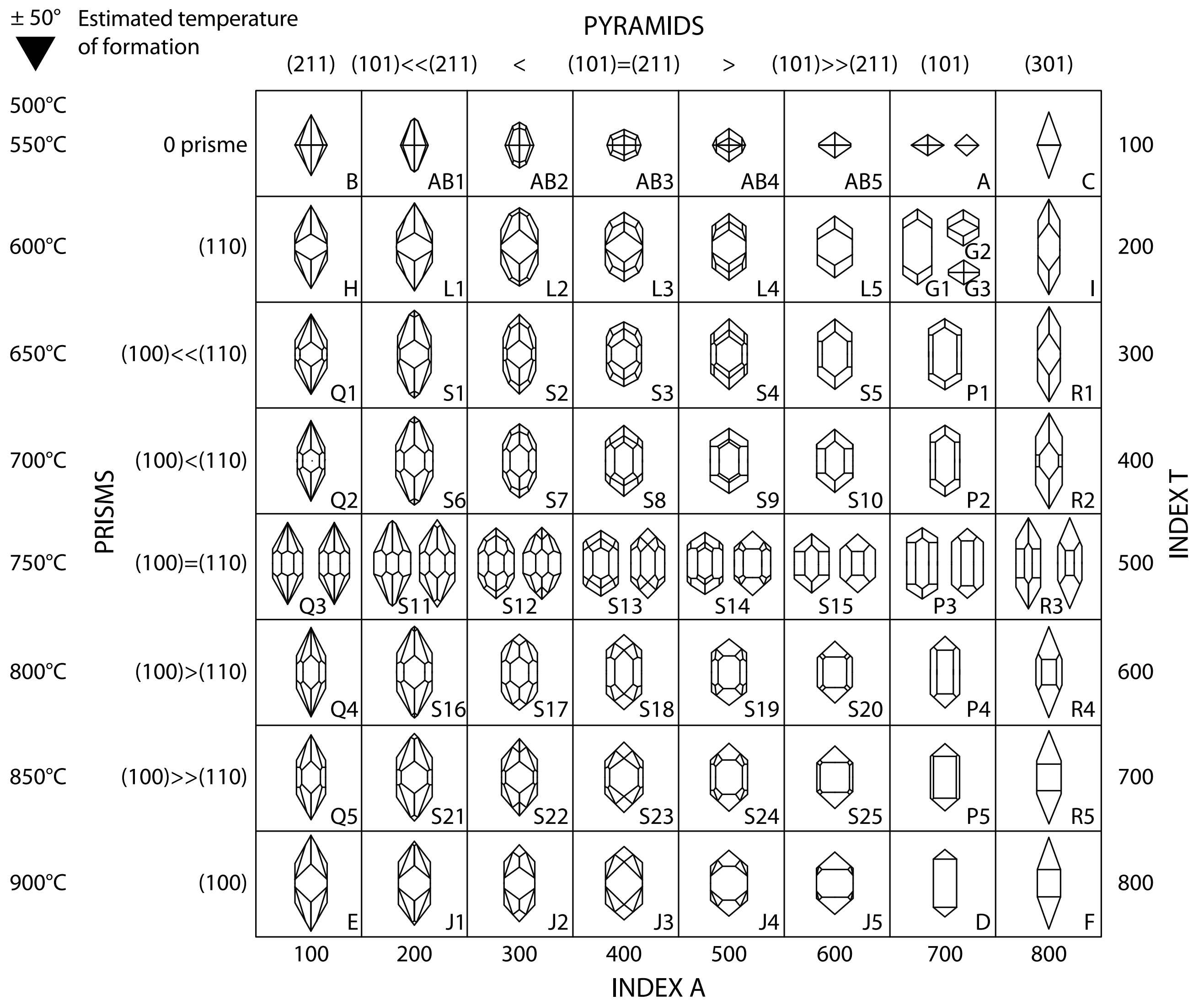

FIGURE 4. Zircon typological classification proposed by Pupin (1980). Index A reflects the Al/alkali ratio, controlling the development of pyramids in the crystals. Index T reflects the effects of temperature on the development of prisms.

Investigaciones en Estratigrafía (IIES) of the Universidad de Caldas (Colombia) using a Nikon LV100® Tri-Polar Pol Universal and PET SMZ1500® stereomicroscope, coupled with a high-resolution Nikon DS-F11® camera. NIS Elements 3.2® software was used for measuring morphometric features. SEM-CL images were obtained using a SEM-Quanta 250® coupled with Chroma CL Gatan® cathodoluminescence device.

All U/Pb measurements were performed by LA-ICPMS (Chang *et al.*, 2006; Schoene, 2014), using a 213nm New Wave Nd: YAG UV laser, coupled to a Thermo-Finnigan Element-2 dual-focus monocollector ICP-MS mass spectrometer. Isotopic measurements were carried out at the University of Arizona's Laser-Chron Laboratory (USA) using the approach proposed by Chang *et al.* (2006).

RESULTS

Zircon morphology and typology

In the following section, we present morphometric characteristics of zircon grains analyzed under optical microscopy.

Zircon roundness and elongation

LJSS zircons fall primarily in the non-rounded or poorly rounded fields 1, 2, 3 and 4 according to Gärtner *et al.* (2013) (Fig. 5A). We note that some crystal faces and edges are still recognizable even when the grains exhibit a degree of roundness, thereby allowing typological characterization (Pupin, 1980). A smaller proportion (~4%) of zircons fall in categories 9

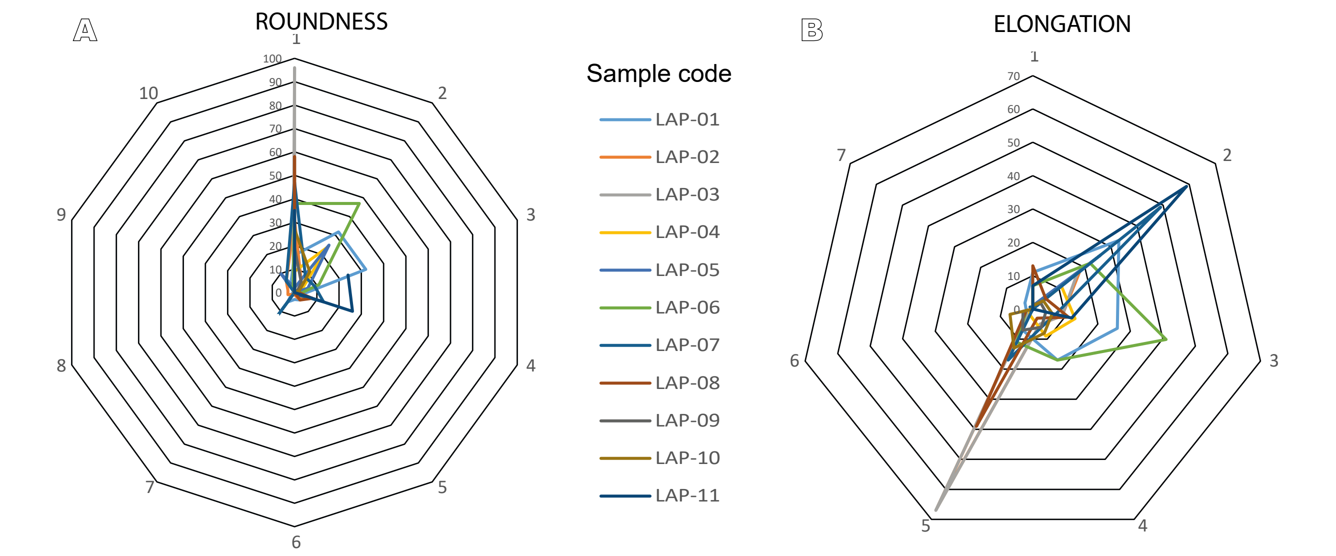

FIGURE 5. Zircon morphological parameters represented in spider diagrams: A) Roundness. B) Elongation. Based on the classification by Gärtner *et al.* (2013).

and 10, corresponding to grains whose faces and some edges are partially recognizable or unrecognizable due to rounding by transport/abrasion (Köster, 1964; Dietz, 1973).

Zircon length varies between ~65 and 500µm, with the majority giving values of ~100µm. Variations in thickness range from ~60 to 250µm. In terms of elongation (Gärtner *et al.*, 2013), most zircons fall within fields 2 and 3 (Fig. 5B) and exhibit length/width ratios between ~1.5 and 2.0. Zircons in the lower portion of this range are classified as low elongation, while maximum values are classified as having moderate elongation (Poldevaart, 1950; Poldervaart, 1955; Hoppe, 1963; Finger and Haunschmid, 1988; Gärtner *et al.*, 2013). Elongation ratios >3 are rare and only occur in significant numbers in two samples (Fig. 5B).

Zircon typology

The different zircon typologies identified in samples analyzed via petrographic and SEM-CL microscopy are shown in Figures 6 and 7. There are few variations in crystal morphologies that were recognized (Fig. 7). Zircons are characterized by high values of A and T indices, and diameters greater than 100µm, thus allowing recognition of crystallographic features.

Zircon crystalline faces are characterized by pyramids {101} and {101} >> {211} and prisms {100} {110} and {100} >> {110}. The typological distribution (Pupin and Turco, 1972a; Pupin, 1980) is similar between most grains (Fig. 7), with P1, P2, P3, P4, and P5 being the most common subtypes (5%-40%). Other subtypes are S5, S10, L5, D (3%-9%). Relatively few grains (1%-3%) fall within the J4 and R5 typologies. Analyzed zircon crystals exhibit a marked homogeneity both in their morphology and optical characteristics (color, degree of transparency, etc.). Due to the homogeneity of the different subtypes, we calculated the mean values of AI and IT for each typology (Fig. 8). These values show that the LJSS zircons are in a mixed field (5 and 6), corresponding to sources of igneous rocks in the granular

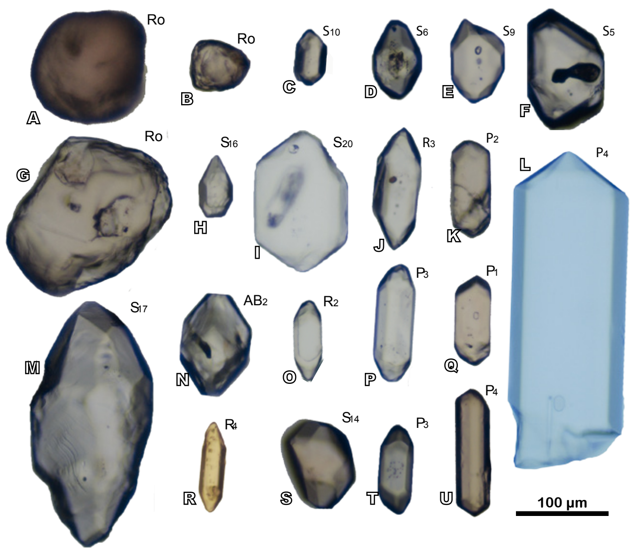

FIGURE 6. Examples of LJSS detrital zircons susceptible to typological analysis. Optical microscopy images taken in extended focus. Letters with index correspond to subtypes of the classification found according to the categories proposed by Pupin (1980) (see Figure 4). Ro: rounded.

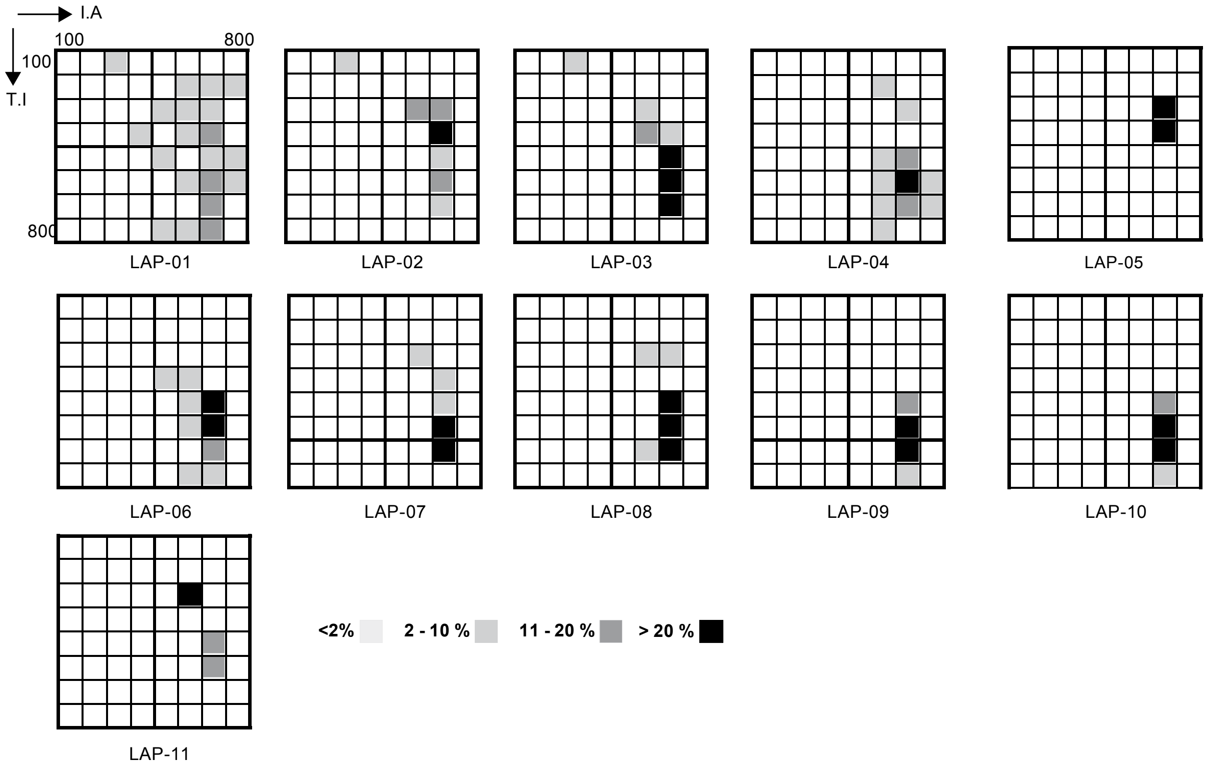

FIGURE 7. Results of the LJSS zircon typology analysis based on the A.I-T.I diagram of Pupin (1980).

subalkaline and alkaline series. Approximately 92% of the zircons are colorless, optically pure (few inclusions, fractures, oxide coatings, etc.). A small proportion (8%) exhibits some degree of coloration, specifically yellow to pale pink. Most mineral inclusions are identified as acicular and/or fine columnar and/or tabular. These are generally oriented along the C axis with a variety of optical shades (colorless, green, brown, etc. (see Fig. 6D, F, I, N, Q).

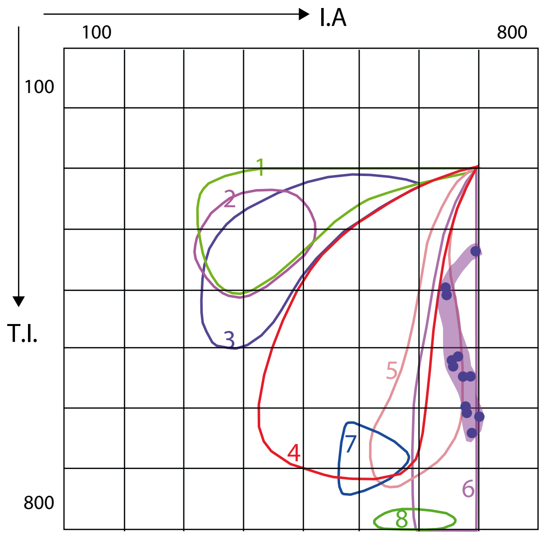

FIGURE 8. Distribution of granitic rocks in the typology diagram derived from the mean value of Al and Tl (Pupin, 1988): 1) alumina leucogranites, 2) monzogranites-granodiorites (sub)autochthonous, 3) monzogranite-granodiorite aluminum intrusives, 4) calc-alkaline and K-rich calc-alkaline series granites, 5) sub-alkaline series granites, 6) alkaline series granites, 7) tholeiitic continental granites, 8) tholeiitic series oceanic granites. Purple points represent the results of zircons analyzed in this study.

Detrital U/Pb dating by LA-ICP-MS

U/Pb dating was performed on 114 individual zircon crystals obtained from a sample at the top of the LJSS (Fig. 9). The results show dominant Miocene peaks (~55% of all dated grains) with absolute ages over tight intervals at approximately 10-13Ma and, the more abundant population (about 60 grains) with ages between ~18-21Ma (Fig. 9). A second age group exhibits Oligocene ages between ~23-31Ma, followed by two Mesozoic clusters with a Cretaceous peak at ~75-82Ma and some zircons with Triassic ages ~230-240Ma. The last age group comprises a small set of zircons (less than 3%) that are older than 500Ma and reach to ~2800Ma. The youngest detrital zircon age population within the Miocene age is interpreted as an estimate of the maximum depositional age for the LJSS in the Tortonian. This date agrees with a biostratigraphically estimated age based on nannofossils assemblages (Vallejo *et al.*, 2016).

Cathodoluminescence images

Dated zircons were analyzed by SEM-CL images, allowing us to identify a variety of internal textures and to establish differences within the age populations. In general, Precambrian zircons have rounded and irregular shapes. In some dated zircons, it was possible to identify their typology to reveal a predominance of subtypes P4 and P5. Internal zircon textures exhibit weak-wide zonation patterns and overlapping zonation domains, as well as some less conspicuous oscillatory zoning patterns (Corfu *et al.*, 2003) (Fig. 10). Mesozoic zircons, which are largely Triassic in age, present a correlation with subtypes such as S10, P2, P3, P4, and P5. Internally, these zircons are characterized by overlapping domains of non-zoned cores surrounded by domains of very fine and strong oscillatory zoning. Finally, Miocene zircons are correlated with a greater variety of S and P typologies, are smaller in size with respect to other populations, and show a better development of crystalline faces. They exhibit varied internal textures including reabsorbed cores with overgrowth, superposition of zonation domains, and fine bimodal zonation (Fig. 10).

DISCUSSION

Applied as integrated provenance analyses, typology and U/Pb geochronology in detrital zircons enables us to constrain the sources of sedimentary material that filled the San Juan Sub-basin during the Miocene. In terms of roundness, the prevalence (91%) of well-faceted to poorly rounded grains indicates that the analyzed zircons were slightly affected by abrasion, suggesting JLSS zircons underwent minimal transport from proximal sources and/or that the kinetic energy during transport was low (Caspers, 1967; Dietz, 1973).

Elongation analysis is a good indicator of potential source rocks (Poldervaart, 1955; Poldervaart, 1956; Hoppe, 1963; List, 1966). In our study, the more elongated zircons are associated with granitic and/or medium- to high-grade metamorphic origins, while short and rounded zircons are linked to reworking or low-grade metamorphism (Poldevaart, 1950; Hoppe, 1963; Finger and Haunschmid, 1988). Elongation is also an indicator of cooling rates, where rapid cooling (*i.e.,* volcanic) generates mostly longer crystals (elongation ratio >3). In this sense, our results show that LJSS zircons do not exhibit a single tendency of elongation. Instead, the majority of crystals analyzed present moderate to high ratios (between ~2 and 3), while two samples give elongation ratios of 5, suggesting that most zircons have an igneous origin characterized by rapid cooling (*e.g.,* shallow intrusions and/or volcanics).

SEM-CL images allow identification of internal textural differences within zircon populations. Precambrian zircons present weak and wide zonation with overlapping domains. Mesozoic zircons display superposition of domains exhibiting non-zoned cores with overgrowth and strong zonation. Such patterns are characteristic of granitic igneous rocks but may also occur in some metamorphic rocks (Corfu *et al.*, 2003). Finally, Miocene zircons are characterized by internal textures exhibiting reabsorbed cores with overgrowth, superposition of zonation domains, and fine bimodal oscillatory zonation (Fig. 10). These textural features are typical of zircons formed in acid to intermediate igneous rocks and develop during zircon crystallization, reflecting processes of reabsorption, precipitation, and crystal growth inside magmatic chambers with compositional variations (Corfu *et al.*, 2003). Zircon typologies in our study indicate that the majority originated from granitic rocks of subalkaline affinity, in addition to

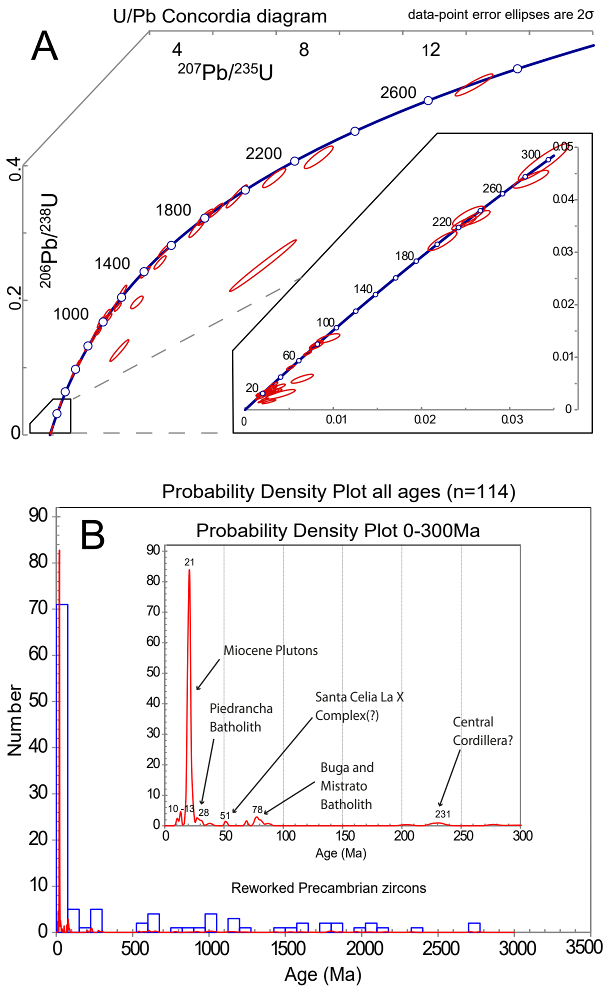

FIGURE 9. U/Pb results for 114 U/Pb dates reported in the detrital zircons for the LJSS sample. A) Concordia Diagram. B) Probability Density Plot (PDP). Larger PDP covers the entire age range reported. Smaller PDP covers ages between 0 and 300Ma where main peaks are marked with the names of some intrusive bodies of the Western Cordillera that fall in these intervals and that are considered as potential sources for detrital material.

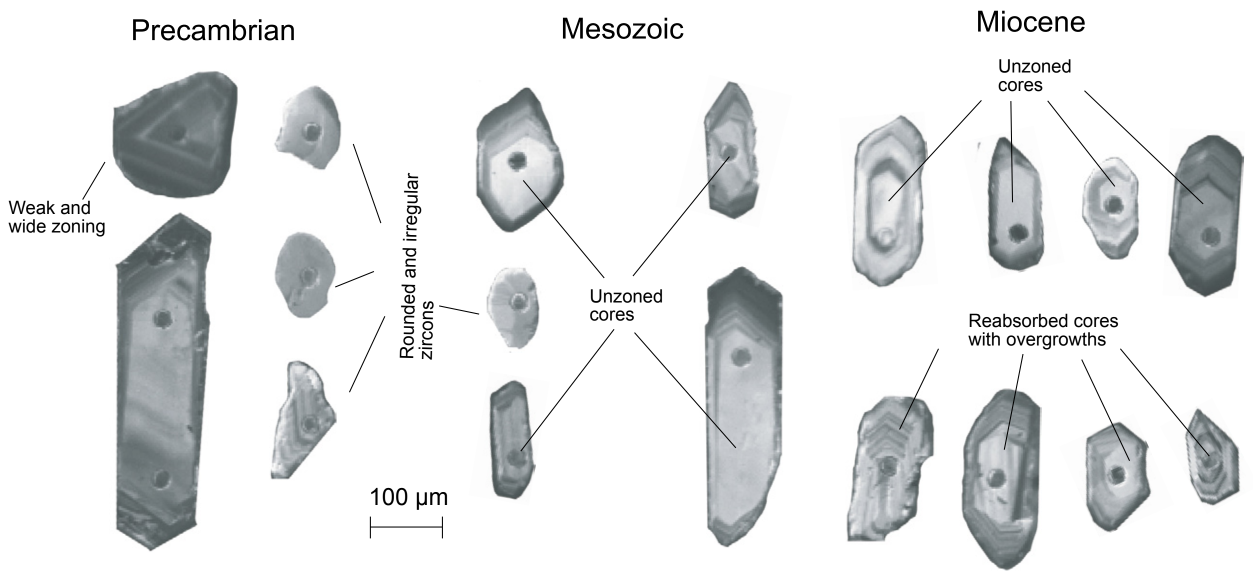

FIGURE 10. Cathodoluminescence (SEM-CL) images of selected LJSS zircons discriminated by age ranges in the Precambrian, Mesozoic and Miocene. Black circles correspond to ablation pits from U/Pb dating.

alkaline granitic rocks (Figs. 7; 8). However, an association of zircon morphology/typology with metamorphic rocks cannot be ruled out.

Detrital zircon populations analyzed for U/Pb ages show age spectra with significant peaks at ca. 10Ma, 12-13Ma, and 18-21Ma (Fig. 9). Less prominent peaks are occur in the intervals ~23-31Ma, ~38-40Ma, ~75-82Ma, and ~230-240Ma. A small proportion of zircons with ages between 500Ma and 2800Ma are also present. Zircons with U/Pb ages in the Burdigalian-Aquitanian interval confirm that material was sourced primarily from plutonic and volcanic rocks of known Miocene age (ca. 18-20Ma), such as the Aguaclara Stock, Danubio Stock, Anchicayá Stock, and Torra Pluton (Brook, 1984; ANH-Universidad de Caldas, 2011). In addition, the younger plutonic Miocene bodies, Serravallian to Tortonian (ca. 10-14Ma), may indicate detrital signatures from northern intrusive sources including the Farallones Batholith, the Horqueta Stock, and other bodies reported by Calle *et al.* (1980), García and García (2012) and Restrepo-Moreno *et al.* (2013). Oligocene U/Pb signatures are attributable to plutons such as the Piedrancha Batholith (Brook, 1984). The contribution of Cretaceous granites can be linked to the Buga Batholith (Villagómez *et al.*, 2011) and the Mistrató Stock (Calle and González, 1982; Moreno-Sanchez and Pardo-Trujillo, 2003). However, the presence of volcanic lithics and hornblende + pyroxene associations (Muñoz and Gomez, 2014), in conjunction with the euhedral and elongated morphology of some zircon grains (elongation ratios >3), with U/ Pb ages predominantly between 10 and 21Ma, are clear indications of volcanic activity during the Miocene depositional stages of the LJSS in western Colombia.

Our results indicate that the primary sources of detrital material for the LJSS correspond to the Late Mesozoic (*i.e.,* Cretaceous) and Cenozoic litho-stratigraphic provinces (Fig. 2), which can be correlated with the present configuration of basement rocks of the western Cordillera. The age ranges reported above are typical of the western Cordillera's plutonic (intermediate to mafic) and volcanic (intermediate) rocks, suggesting that this mountain range was already a significant topographic barrier, with exposed and geomorphically active crystalline massifs. Conversely, Triassic to Precambrian zircons are often associated with crystalline rocks of the central Cordillera (Horton *et al.*, 2015; Nie *et al.*, 2010; Vinasco *et al.*, 2006). The presence of a few zircon grains in this U/Pb age-range, with typical peaks at ~230-250Ma, 600Ma, 900-1000Ma, etc., does not necessarily imply a direct fluvial connection between the central Cordillera and sedimentary formations along the Pacific coast. We interpret such zircons as being derived from reworking of Cretaceous sedimentary covers positioned over the western Cordillera (*e.g.,* Penderisco Formation, Urrao Member) where populations with these Paleozoic and Precambrian ages have been reported (*i.e.,* polycyclic zircons; ANH-Universidad de Caldas, 2011).

Based on the presence of Cretaceous zircons in the LJSS, it could be argued that, since the central Cordillera also exhibits considerable pulses of Cretaceous magmatism (Restrepo-Moreno *et al.*, 2009; Villagómez and Spikings, 2013; Cochrane *et al.*, 2014), the possibility of a fluvial connection between the central Cordillera and the LJSS should not be discounted. Yet, the absence of Jurassic U/ Pb ages from the SSJL is notable, despite of the fact that there are plutonic masses of considerable size and Jurassic age in the central Cordillera, such as the Ibague Batholith (Gómez *et al.*, 2015), positioned at almost the same latitude as the SSJL.

Relative to the PCB, the virtual absence of Eocene zircons in the interval ~38-50Ma, corresponding to some intrusives typical of the Panamanian Arc (*e.g.*, Mandé Batholith (Botero, 1981; Villagómez and Spikings, 2013) and/or the Acandí Batholith (Álvarez and Parra, 1971; Sillitoe *et al.*, 1982), would indicate that: i) the PCB was still in a distal position with respect to the LJSS at 10Ma, ii) Mandé-like plutonic units were still unexposed massifs (*i.e.,* in subsurficial positions and in the process of exhumation) and thus did not contribute sediments to the basin and/or iii) there was no fluvial network connecting geomorphically active Panamanian elements with the LJSS. However, recent studies indicate that the plutonic masses of the Panamanian Arc were already exhumed and served as source areas for sedimentary formations in Panamá (Ramírez *et al.*, 2016), making options i) and iii) above more reasonable.

The prevalence of western Cordillera-like zircon detrital signatures (based on U/Pb age and typologies, this study), the dominant heavy mineral fractions for these sediments (Muñoz and Gómez, 2014) and the absence of significant zircon U/Pb age signals older than the Cretaceous can be considered as preliminary evidence for the topographic control exerted by the western Cordillera hindering fluvial connections between the central Cordillera and the LJSS. In addition, the presence of zircons potentially derived from Miocene plutonic bodies (*e.g.,* Farallones Stock, Tatamá Pluton, etc.) located north and east of the LJSS, and on an axial portion on the western Cordillera, indicates that such plutons were exhumed and geomorphically active and thereby formed areas of detrital contribution within the paleofluvial network. Further to this detrital-fluvial contribution, we suggest there may have been a significant direct contribution from the volcanic products of a Miocene magmatic arc.

Based on our results, a feasible paleogeographic reconstruction shows that during the time of LJSS sedimentation (Burdigalian-Tortonian) there was a

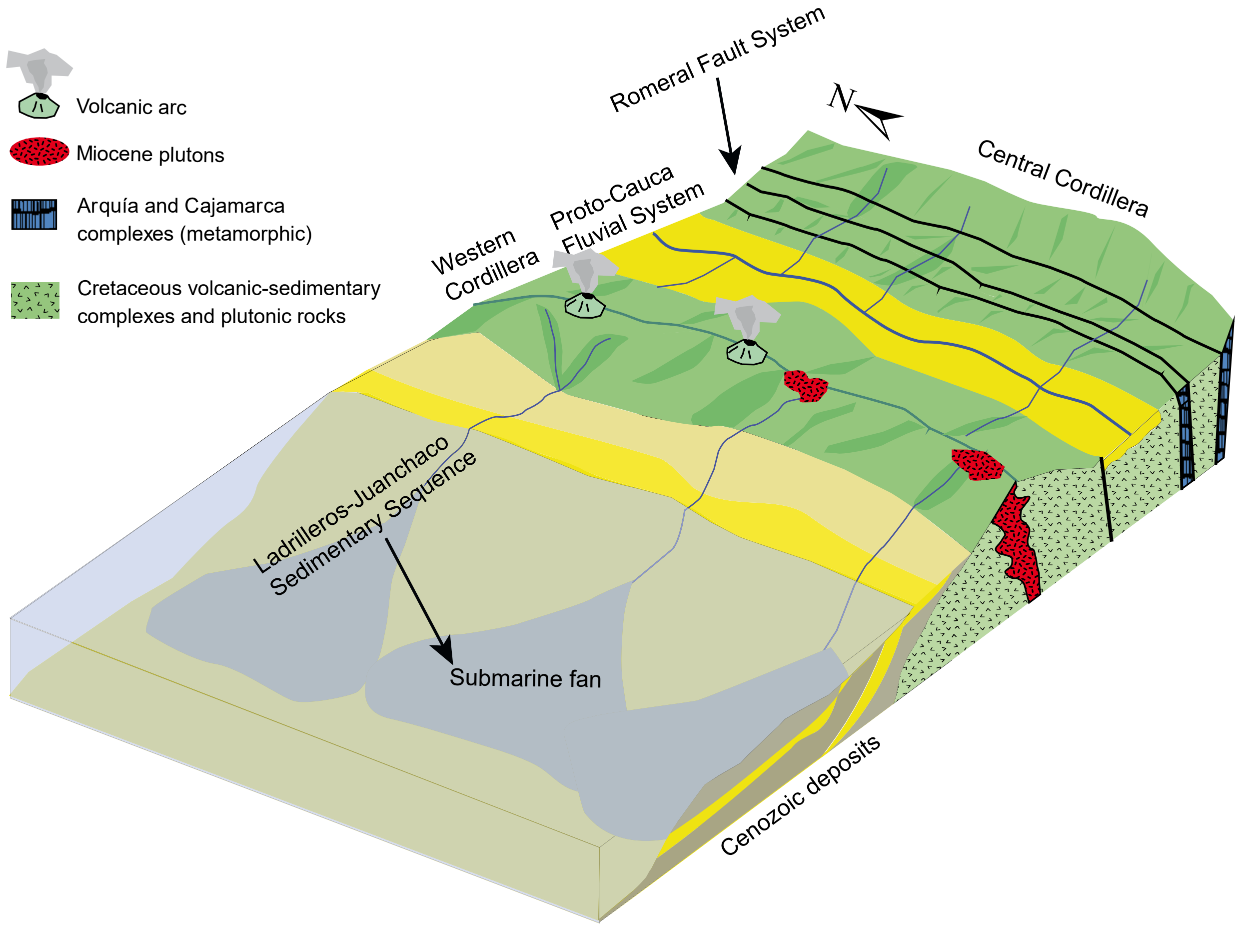

FIGURE 11. Paleogeographic model for the LJSS, Proto-Cauca fluvial system and western cordillera during the Miocene (Burdigalian-Tortonian). Colors are only a reference to differentiate environments and lithologies and do not represent geologic time.

volcanic-magmatic arc in the western Cordillera of sufficient topographic relief to separate central Cordillera source areas from Pacific basins. Marked pulses of uplift and erosional exhumation are also reported for the western Cordillera for the interval 15-9Ma (Restrepo-Moreno *et al.*, 2015). As in present times, this topographic barrier played a pivotal role for a river network restricted to the western flank of the western Cordillera that controlled the extent of fluvial dissection, erosion, and sediment production-routing into the Pacific plains (Fig. 11). The proposition of an already existing western Cordillera as a considerable topographic barrier since the middle Miocene is consistent with determinations, based on evidence from borehole and seismic data, on the extent of Pacific basins in Colombia (*i.e.,* those situated to the west of the western Cordillera) that show significant reduction in thickness as one moves from west to east (*i.e.,* from the Pacific Ocean to the western Cordillera).

CONCLUSIONS

Integration of techniques such as detrital zircon typology/morphometry, U/Pb dating, and SEM-CL imaging in samples from the LJSS arenites affords improved constraint of the depositional age and provenance of the terrigenous materials deposited in the basin during the Burdigalian-Tortonian. The high affinity of the zircons (typology/age/internal zonation patterns) with Miocene igneous rocks (plutonic and volcanic) potentially implies that an active volcanic-magmatic arc with significant topography existed in the western Cordillera and was the main sediment source. Detrital sources on the central Cordillera were separated from the Pacific realm by well-established western Cordillera topographic barriers.

Our methodological approach to evaluate provenance in a complex litho-structural regime represents a viable development of the standard methodology, considering the quantity of information provided in provenance studies and paleogeographic reconstruction, and should be systematically used in other sedimentary sequences in the northern Andes.

ACKNOWLEDGMENTS

This work was carried out with support from the Instituto de Investigaciones en Esratigrafía (IIES) and the Research Group in Stratigraphy and Volcanology (GIEV-Cumanday) at Universidad de Caldas (Colombia). Institutional support from the National Hydrocarbons Agency (ANH, Colombia), Universidad Nacional de Colombia Sede Medellín. We are grateful to the personnel at the LaserCrhon Laboratory of the University of Arizona. We greatly appreciate the comments and suggestions from Yamirka Rojas-Agramonte and Javier Fernández-Suárez, whose input significantly improved the quality of the manuscript.

REFERENCES

Álvarez, E., Parra, E., 1971. Evaluación del prospecto de cobre y molibdeno en las cabeceras del Río Muerto. Municipio de Acandí, Departamento Del Chóco: Ingeominas, Informe, 30, 1-180.

Anani, C., Tateishi, M., Asiedu, D., Atta-Petters, D., Manu, J., 2012. Zircon Typology as Indicator of Provenance in Neoproterozoic Sandstones of the Voltaian Basin, Ghana. Research Journal of Environmental and Earth Sciences, 4(2), 151-161.

Agencia Nacional de Hidrocarburos (ANH)-Universidad de Caldas, 2011. Estudio geológico integrado en la Cuenca Tumaco Onshore. Síntesis cartográfica, sísmica y análisis bioestratigráfico, petrográfico, geocronológico, termocronológico y geoquímico de testigos de perforación y muestras de superficie. Informe contrato 092, ANH, unpublished, 234pp.

Armstrong-Altrin, J.S., Yong II, L., Surendra, P.V., Ramasamy, S., 2004. Geochemistry of Sandstones from the Upper Miocene Kudankulam Formation, Southern India: Implications for Provenance, Weathering, and Tectonic Setting. Journal of Sedimentary Research, 74(2), 285-297.

Bayona, G., Montes, C., Cardona, A., Jaramillo, C., Ojeda, G., Valencia, V., Ayala-Calvo, C., 2011. Intraplate subsidence and basin filling adjacent to an oceanic arc-continent collision: a case from the southern Caribbean-South America plate margin. Basin Research, 23(4), 403-422. DOI: 10.1111/j.1365-2117.2010.00495.x

Belousova, E.A., Griffin, W.L., O'Reilly, S.Y., 2005. Zircon Crystal Morphology, Trace Element Signatures and Hf Isotope Composition as a Tool for Petrogenetic Modelling: Examples From Eastern Australian Granitoids. Journal of Petrology, 47(2), 329-353. DOI: 10.1093/petrology/egi077

Bernet, M., Spiegel, C., 2004. Detrital thermochronology. Geological Society of America Bulletin, 378, 1-6.

Boggs, S., 2009. Petrology of Sedimentary Rocks. New York, Cambridge University Press, 612pp.

Botero, G., 1981. Edades radiométricas de algunos plutones colombianos. Boletín de Ciencias de la Tierra. Universidad Nacional de Colombia, 5(6), 135-143.

Bowring, S.A., Schmitz, M.D., 2003. High-Precision U-Pb Zircon Geochronology and the Stratigraphic Record. Reviews in Mineralogy and Geochemistry, 53(1), 305-326.

Brook, M., 1984. New age radiometric data from SW Colombia. INGEOMINAS - Misión Britanica, 10, 1-25.

Calle, B., González, H., 1982. Geología y Geoquímica de la Plancha 186 Riosucio. Medellín, INGEOMINAS Informe 1878, 124pp.

Calle, B., Toussaint, J.F., Restrepo, J.J., Linares, E., 1980. Edades K/Ar de dos plutones de la parte septentrional de la Cordillera Occidental, Colombia. Geología Norandina, 2, 17-20.

Carrapa, B., 2010. Resolving tectonic problems by dating detrital minerals. Geology, 38(10), 91-92.

Caspers, H., 1967. Erhard Köster: Granulometrische und morphometrische Meßmethoden an Mineralkörnern, Steinen und sonstigen Stoffen. Mit 109 Abb., 68 Tafeln. Stuttgart: Ferdinand Enke Verlag 1964. 336 S. Geb. 63.–DM. Internationale Revue Der Gesamten Hydrobiologie Und Hydrographie, 52(4), 656-656. DOI: 10.1002/iroh.19670520420

Cediel, F., Shaw, R.P., Cáceres, C., 2003. Tectonic assembly of the Northern 549 Andean Block. In: Bartolini, C., Buffler, R.T., Blickwede, J. (eds.). The 550 Circum Gulf of Mexico and the Caribbean: Hydrocarbon habitats, basin formation, and plate tectonics. American Association of Petroleum Geologists (AAPG), 79 (Memoir), 815-848.

Cediel, F., Restrepo, I., Marín-Cerón, M.I., Duque-Caro, H., Cuartas, C., Mora, C., Muñoz, G., 2009. Geology and Hydrocarbon Potential, Atrato and San Juan Basins, Chocó (Panamá) Arc. Tumaco Basin (Pacific Realm). Medellin (Colombia), Fondo editorial Universidad EAFIT, 178pp.

Chang, Z., Vervoort, J.D., McClelland, W.C., Knaack, C, 2006. U-Pb dating of zircon by LA-ICP-MS. Geochemistry, Geophysics, Geosystems, 7(5), 1-14 DOI: 10.1029/2005GC001100

Cochrane, R., Spikings, R., Gerdes, A., Ulianov, A., Mora, A., Villagómez, D., Chiaradia, M., 2014. Permo-Triassic anatexis, continental rifting and the disassembly of western Pangaea. Lithos, 190, 383-402. DOI: 10.1016/j.lithos.2013.12.020

Corfu, F., Hanchar, J.M., Hoskin, P.W.O., Kinny, P., 2003. Atlas of Zircon Textures. In: Hanchar, J.M., Hoskin, P.W.O. (eds.). Zircon. Mineralogical Society of America Geochemical Society, 53, 469-500.

Dabard, M.P., Loi, A., Peucat, J.J., 1996. Zircon typology combined with Sm/Nd whole-rock isotope analysis to study Brioverian sediments from the Armorican Massif. Sedimentary Geology, 101(3–4), 243-260. DOI: 10.1016/0037-0738(95)00068-2

Davis, D.W., Williams, I.S., Krogh, T.E., 2003. Historical development of zircon geochronology. In: Hanchar, J.M., Hoskin, P.W.O. (eds.). Zircon. Mineralogical Society of America Geochemical Society, 53, 146-181.

Dickinson, W.R., 1985. Interpreting provenance relations from detrital modes of sandstones. In: Zuffa, E.G.G. (ed.). Provenance of arenites. Dordrecht, D. Reidel Publishing Company, 333-361.

Dietz, V., 1973. Experiments on the influence of transport on shape and roundness of heavy minerals. Contributions to Sedimentology, 1, 69-102.

Dostal, J., Keppie, J.D., 2009. Geochemistry of low-grade clastic rocks in the Acatlán Complex of southern Mexico: Evidence for local provenance in felsic–intermediate igneous rocks. Sedimentary Geology, 222(3), 241-253. DOI: 10.1016/j.sedgeo.2009.09.011

Duque-Caro, H., 1990. The Choco Block in the northwestern corner of South America: Structural, tectonostratigraphic, and paleogeographic implications. Journal of South American Earth Sciences, 3(1), 71-84.

Etemad-Saeed, N., Hosseini-Barzi, M., Armstrong-Altrin, J.S., 2011. Petrography and geochemistry of clastic sedimentary rocks as evidences for provenance of the Lower Cambrian Lalun Formation, Posht-e-badam block, Central Iran. Journal of African Earth Sciences, 61(2), 142-159. DOI: 10.1016/j.jafrearsci.2011.06.003

Farris, D.W.C., Restrepo-Moreno, S.A., Jaramillo, C., Bayona, G., Montes, C., Cardona, A., Reiners, P., Mora, A., Speakman, R.J., Glasscock, M.D., 2011. Evolution of the Panamanian Isthmus. Geology, 39(11), 10071010.

Fedo, C.M., Sircombe, K.N., Rainbird, R., 2003. Detrital zircon analysis of the sedimentary record. In: Hanchar, J.M., Hoskin, P.W.O. (eds.). Zircon. Mineralogical Society of America Geochemical Society, 53, 277-303.

Finch, R.J., Hanchar, J.M., 2003. Structure and Chemistry of Zircon and Zircon-Group Minerals. Reviews in Mineralogy and Geochemistry, 53(1), 1-25. DOI: 10.2113/0530001

Finger, F., Haunschmid, B., 1988. Die mikroskopische Untersuchung der akzessorischen Zirkone als Methode zur Klärung der Intrusionsfolge in Granitgebieten-eine Studie im nordöstlichen oberösterreichischen Moldanubikum. Jb. Geologische Bundesanslat, 131(2), 255-256.

García, G.R., García, G.Z., 2012. Características del plutonismo Mioceno superior en el segmento norte de la Cordillera Occidental e implicaciones tectónicas en el modelo geológico del noroccidente colombiano. Boletín de Ciencias de la Tierra, 31, 5-22.

Gärtner, A., Linnemann, U., Sagawe, A., Hofmann, M., Ullrich, B., Kleber, A., 2013. Morphology of zircon crystal grains in sediments-characteristics, classifications, definitions. Geologica Saxonica, 59, 65-73.

Garver, J.I., 2014. Thermochronology, Detrital Zircon. In: Rink, J.W., Thompson, J. (eds.) Encyclopedia of Scientific Dating Methods. Dordrecht, Springer Netherlands, 1-7.

Garzanti, E., Baud, A., Mascle, G., 1987. Sedimentary record of the northward flight of India and its collision with Eurasia (Ladakh Himalaya, India). Geodinamica Acta, 1(4-5), 297-312. DOI: 10.1080/09853111.1987.11105147

Garzanti, E., Critelli, S., Ingersoll, R.V., 1996. Paleogeographic and paleotectonic evolution of the Himalayan Range as reflected by detrital modes of Tertiary sandstones and modern sands (Indus transect, India and Pakistan). Geological Society of America Bulletin, 108(6), 631-642. DOI: 10.1130/0016-7606(1996)108<0631:PAPEOT>2.3.CO;2

Garzanti, E., Doglioni, C., Vezzoli, G., Andò, S., 2007. Orogenic Belts and Orogenic Sediment Provenance. The Journal of Geology, 115(3), 315-334. DOI: 10.1086/512755

Gehrels, G., 2012. Detrital Zircon U-Pb Geochronology: Current Methods and New Opportunities. In: Busby, C., Azor Pérez, A. (eds.). Tectonics of Sedimentary Basins: Recent Advances. Chichester (United Kingdom), John Wiley & Sons, 664pp. DOI: 10.1002/9781444347166.ch2

Gehrels, G., 2014. Detrital Zircon U-Pb Geochronology Applied to Tectonics. Annual Review of Earth and Planetary Sciences, 42(1), 127-149. DOI: 10.1146/annurev-earth-050212-124012

Gómez, J., Nivia, Á., Montes, N.E., Almanza, M.F., Alcárcel, F.A., Madrid, C.A., 2015. Compilando la geología de Colombia: Una visión a 2015. In: Gómez Tapias, J., Almaza Meléndez, M.F. (eds.). Bogotá. Servicio Geológico Colombiano, Publicaciones Geológicas Especiales, 33, 429pp.

González, J.L., Correa, I.D., 2001. Late Holocene Evidence of Coseismic Subsidence on the San Juan Delta, Pacific Coast of Colombia. Journal of Coastal Research, 17(2), 459-467.

Grimes, C.B., Wooden, J.L., Cheadle, M.J., John, B.E., 2015. «Fingerprinting» tectono-magmatic provenance using trace elements in igneous zircon. Contributions to Mineralogy and Petrology, 170(5-6), 1-26. DOI: 10.1007/s00410-015-1199-3

Hanchar, J.M., Hoskin, P.W.O, 2003. Reviews in Mineralogy and Geochemistry. In: Hanchar, J.M., Hoskin, P.W.O. (eds.). Zircon. Mineralogical Society of America Geochemical Society, 53, 1-10.

Hanchar, J.M., Rudnick, R.L., 1995. Revealing hidden structures: The application of cathodoluminescence and back-scattered electron imaging to dating zircons from lower crustal xenoliths. Lithos, 36(3), 289-303.

Hoppe, G., 1963. Die Verwendbarkeit morphologischer Erscheinungen an akzessorischen Zirkonen für petrogenetische Auswertungen. Akademie-Verlag, 1, 1-23.

Horton, B.K., Anderson, V.J., Caballero, V., Saylor, J.E., Nie, J., Parra, M., Mora, A., 2015. Application of detrital zircon U-Pb geochronology to surface and subsurface correlations of provenance, paleodrainage, and tectonics of the Middle Magdalena Valley Basin of Colombia. Geosphere, 11(6), 1790-1811.

Kellogg, J.N., 1984. Cenozoic tectonic history of the Sierra de Perijá, Venezuela-Colombia, and adjacent basins. Geological Society of America Bulletin, 162, 239-262.

Kellogg, J.N., Bonini, W.E., 1982. Subduction of the Caribbean plate and basement uplifts in the overriding South American plate. Tectonics, 1(3), 251-276.

Košler, J., Sylvester, P.J., 2003. Present trends and the future of zircon in geochronology: laser ablation ICPMS. Reviews in Mineralogy and Geochemistry, 53(1), 243-275.

Köster, E., 1964, Granulometrische und morphometrische Meßmethoden an Mineralkörnern. Steinen und sonstigen Stoffen, 336pp.

List, F.K., 1966. Statistische Untersuchungen an Zirkon und Apatit in Anatexiten des südlichen Bayerischen Waldes. Geologische Rundschau, 55(2), 509-530. DOI: 10.1007/BF01765788

Loi, A., Dabard, M.P., 1997. Zircon typology and geochemistry in the palaeogeographic reconstruction of the Late Ordovician of Sardinia (Italy). Sedimentary Geology, 112(3), 263-279.

Mange, M.A., Wright, D.T., 2007. Heavy minerals in use. Amsterdam, Elsevier, 58, 1329pp.

Montoya, A., 2003. Geología de las planchas 240, 241, 259 and 260. Bogotá, Ingeominas, 180pp.

Montes, C., Cardona, A., Jaramillo, C., Pardo, A., Silva, J.C., Valencia, V., Ayala, C., Pérez-Angel, L.C., Rodriguez-Parra, L.A., Ramirez, V., 2015. Middle miocene closure of the Central American seaway. Science, 348(6231), 226-229.

Moreno-Sanchez, M., Pardo-Trujillo, A., 2003. Stratigraphical and sedimentological constraints on western Colombia: Implications on the evolution of the Caribbean plate. In: Bartolini, C., Buffler, R.T., Blickwede, J. (eds.). The Circum-Gulf of Mexico and the Caribbean: Hydrocarbon habitats, basin formation, and plate tectonics. American Association of Petroleum Geologists. Memories, 79, 891-924.

Muñoz, A., Gómez, L., 2014. Procedencia de las arenitas de la sección Juanchaco-Ladrilleros (Mioceno, Pacifico colombiano). B.Sc. Thesis. Manizales Colombia, Universidad de Caldas, Unpublished, 75pp.

Nivia, Á., 1996. El Complejo Estructural Dagua, registro de deformación de la Provincia Litosférica Oceánica Cretácica Occidental. Bogotá (Colombia), VII Congreso Colombiano de Geología, Memorias, 54-67.

O'Dea, A., Lessios, H.A., Coates, A.G., Eytan, R.I., Restrepo-Moreno, S.A., Cione, A.L., Jackson, J.B.C., 2016. Formation of the Isthmus of Panama. Science Advances, 2(8), 1-12. DOI: 10.1126/sciadv.1600883

Pettijohn, F., 1975. Sedimentary Rocks. New York, Harper and Row, 3rd edition, 628pp.

Pindell, J.L., Kennan, L., 2013. Tectonic evolution of the Gulf of Mexico, Caribbean and northern South America in the mantle reference frame: an update. London, Geological Society, 328(1, Special Publications), 1-55. DOI: 10.1144/SP328.1

Pindell, J., Kennan, L., Maresch, W.V, Stasnek, K.-P., Draper, G., Higgs, R., 2005. Plate Kinematic and crustal dynamics of circum-Caribbean arc continent interactions: Tectonics controls on basin development in the Proto-Caribbean margins. In: Avé-Lallemant, H.G., Sisson, V.B. (eds.). Caribbean-South American Plate Interactions. Geological Society of America, 394 (Special Papers), 7-52.

Poldervaart, A., 1950. Variation of optical properties with composition in the Forsterite-Fayalite series. American Mineralogist, 35(11-1), 1067-1079.

Poldervaart, A., 1955. Zircons in rocks; part 1, sedimentary rocks; part 2, igneous rocks. American Journal of Science, 253(8), 433-461.

Poldervaart, A., 1956. Zircon in rocks; 2, Igneous rocks. American Journal of Science, 254(9), 521-554. DOI: 10.2475/ajs.254.9.521

Pupin, J.P., 1980. Zircon and granite petrology. Contributions to Mineralogy and Petrology, 73(3), 207-220. DOI: 10.1007/BF00381441

Pupin, J.P, 1988. Granites as indicators in paleogeodynamics. Rendiconti della Societa Italiana di Mineralogia e Petrologia, 43(2), 237-262.

Pupin, J.P., Turco, G., 1972a. Le zircon accessoire en géothermométrie. Comptes Rendus de l'Académie des Sciences, 274(2), 212-214.

Pupin, J.P., Turco, G., 1972b. Une typologie originale du zircon accessoire. Bulletin de la Société Française de Minéralogie, 95, 348-359.

Pupin, J.-P., Minéraux, C., 1976. Signification des caractères morphologiques du zircon commun des roches en pétrologie:

base de la méthode typologique, applications. Doctoral Thesis. Université de Nice, Laboratoire de pétrologie-minéralogie, 394pp.

Pupin, J.P., Bonin, B., Tessier, M., Turco, G., 1978. Role de l'eau sur les caracteres morphologiques et la cristallisation du zircon dans les granitoides. Bulletin de la Société Géologique de France, 5, 721-725. DOI: 10.2113/gssgfbull.S7-XX.5.721

Ramírez, D.A., Foster, D.A., Min, K., Montes, C., Cardona, A., Sadove, G., 2016. Exhumation of the Panama basement complex and basins: Implications for the closure of the Central American seaway. Geochemistry, Geophysics, Geosystems, 17(5), 1758-1777. DOI: 10.1002/2016GC006289

Reiners, P.W., Ehlers, T.A., Zeitler, P.K., 2005. Past, Present, and Future of Thermochronology. In: Reiners, P.W., Ehlers, T.A. (eds.). Low-temperature thermochronology: techniques, interpretations, and applications. Reviews in Mineralogy and Geochemistry, 58, 49-94.

Restrepo, J.J., Toussaint, J.F., 1988. Terranes and continental accretion in the Colombian Andes. Episodes, 11(3), 189-193.

Restrepo-Moreno, S.A., Foster, D.A., O'Sullivan, P., Donelick, R.A., Stockli, D.F., 2009. Cenozoic exhumation of the Antioqueño Plateau, Northern Andes, Colombia, from apatite low-temperature thermochronology. Eos transactions, American Geophysical Union (AGU) publications, 90(52, Fall Meeting Supplement), Abstract T43B-2091.

Restrepo-Moreno, S., Min, K., Bernet, M., Barbosa, A., Marín-Cerón, M., Juliana, J., Hardwick, E., Pardo, A., 2013. Thermotectonic history of the Farallones del Citará batholith (Colombia's Western Cordillera) through multi-system, vertical profile thermochronology/geochronology: tectonic, geomorphic and climatic implications. Colombia, XIV Congreso Colombiano de Geología, Primer simposio de exploradores, 577pp.

Restrepo-Moreno, S., Vinasco, C., Foster, D., Noriega, S., Bernet, M., Marín-Cerón, M., Botero, M., 2015. Cenozoic accretion and morpho-tectonic response in the Northern Andes (Colombia) through low-temperature thermochronology analyses/modeling. Maryland (Baltimore), Geological Society of America (GSA) annual metting, 675pp.

Schoene, B., 2014. 4.10–U–Th–Pb geochronology. Treatise on Geochemistry, Elsevier Ltd., 4, 341-378.

Shahbazi, H., Salami, S., Siebel, W., 2014. Genetic classification of magmatic rocks from the Alvand plutonic complex, Hamedan, western Iran, based on zircon crystal morphology. Chemie der Erde - Geochemistry, 74(4), 577-584. DOI: 10.1016/j.chemer.2013.11.001

Sillitoe, R., Jaramillo, L., Damon, P.E., Shafiqullah, M., Escovar, R., 1982. Setting, charasteristics, and age of the Andean porphyry copper belt in Colombia. Economic Geology, 77, 1837-1850.

Solari, L., Tanner, M., 2011. U-Pb age, a fast data reduction script for LA-ICP-MS U-Pb geochronology. Revista Mexicana de Ciencias Geológicas, 28(1), 83-91.

Spikings, R.A., Winkler, W., Seward, D., Handler, R., 2001. Along-strike variations in the thermal and tectonic response of the continental Ecuadorian Andes to the collision with heterogeneous oceanic crust. Earth and Planetary Science Letters, 186(1), 57-73. DOI: 10.1016/s0012-821x(01)00225-4

Taboada, A., Rivera, L.A., Fuenzalida, A., Cisternas, A., Philip, H., Bijwaard, H., Olaya, J., Rivera, C., 2000. Geodynamics of the northern Andes: subductions and intracontinental deformation. Tectonics, 19(5), 787-813.

Thomas, W.A., 2011. Detrital-zircon geochronology and sedimentary provenance. Lithosphere, 3(4), 304-308. DOI: 10.1130/RF.L001.1

Toussaint, J.F., 1995. Evolución geológica de Colombia. Medellín, Universidad Nacional de Colombia sede Medellín, 166pp.

Vallejo, D.F., Flores, J.A., Plata, A., Trejos, R., Pardo, A., Sierro, F.J., Bárcena, M.A., 2016. Low-latitude Miocene calcareous and siliceous microfossil biostratigraphy from NW of South America. Ladrilleros-Juanchaco section, Colombian Pacific. Ameghiniana, 53(6), 629-644.

Velez, M.I., Hooghiemstra, H., Metcalfe, S., 2005. Fossil and modern diatom assemblages from the Savanna Lake El Pinal, Colombia: An environmental reconstruction. Diatom Research, 20(2), 387-407.

Villagómez, D., Spikings, R., 2013. Thermochronology and tectonics of the Central and Western Cordilleras of Colombia: Early Cretaceous–Tertiary evolution of the Northern Andes. Lithos, 160, 228-249. DOI: 10.1016/j.lithos.2012.12.008

Villagómez, D., Spikings, R., Magna, T., Kammer, A., Winkler, W., Beltrán, A., 2011. Geochronology, geochemistry and tectonic evolution of the Western and Central cordilleras of Colombia. Lithos, 125(3–4), 875-896. DOI: 10.1016/j.lithos.2011.05.003

Willner, A.P., Sindern, S., Metzger, R., Ermolaeva, T., Kramm, U., Puchkov, V., Kronz, A., 2003. Typology and single grain U/Pb ages of detrital zircons from Proterozoic sandstones in the SW Urals (Russia): early time marks at the eastern margin of Baltica. Precambrian Research, 124(1), 1-20. DOI: 10.1016/S0301-9268(03)00045-7

Zoleikhaei, Y., Frei, D., Morton, A., Zamanzadeh, S.M., 2016. Roundness of heavy minerals (zircon and apatite) as a provenance tool for unraveling recycling: A case study from the Sefidrud and Sarbaz rivers in N and SE Iran. Sedimentary Geology, 342, 106-117. DOI: 10.1016/j.sedgeo.2016.06.016

Manuscript received December 2016;
revision accepted May 2017;
published Online July 2017.